行政院國家科學委員會專題研究計畫 期中進度報告

以小鼠模式探討免疫及病毒引發之登革出血機制(1/3)
期中進度報告(完整版)

計 畫 類 別 ：個別型
計 畫 編 號 ：NSC 95-3112-B-002-027-
執 行 期 間 ：95 年 05 月 01 日至 96 年 07 月 31 日
執 行 單 位 ：國立臺灣大學醫學院免疫學研究所

計 畫 主 持 人：伍安怡

處 理 方 式 ：本計畫涉及專利或其他智慧財產權，1 年後可公開查詢

中 華 民 國 96 年 03 月 26 日

行政院國家科學委員會補助專題研究計畫 ☑ 成 果 報 告 □期中進度報告

以小鼠模式探討免疫及病毒引發之登革出血機制

計畫類別：☑ 個別型計畫　　□ 整合型計畫
計畫編號：NSC 95－3112－B－002－027－
執行期間：95 年 05 月 01 日至 96 年 07 月 31 日

計畫主持人：伍安怡
共同主持人：
計畫參與人員：陳萱靜，嚴玉婷，林榮辰，林洋鼎

成果報告類型(依經費核定清單規定繳交)：□精簡報告　☑完整報告

本成果報告包括以下應繳交之附件：
□赴國外出差或研習心得報告一份
□赴大陸地區出差或研習心得報告一份
□出席國際學術會議心得報告及發表之論文各一份
□國際合作研究計畫國外研究報告書一份

處理方式：除產學合作研究計畫、提升產業技術及人才培育研究計畫、列管計畫及下列情形者外，得立即公開查詢
☑涉及專利或其他智慧財產權，☑一年□二年後可公開查詢

執行單位：

中　華　民　國　　96 年　　3 月　　21 日

Full title: Both Virus and TNF-α are Critical in Endothelium Damage in a Dengue Virus-Induced Hemorrhage Mouse Model

Running title: BOTH DV AND TNF-α ARE CRITICAL IN ENDOTHELIUM DAMAGE

Hsuen-Chin Chen,[1] Florence M. Hofman,[2] John T. Kung,[3] Yang-Ding Lin,[1] and Betty A. Wu-Hsieh[1*]

Graduate Institute of Immunology, National Taiwan University, College of Medicine, Taipei, Taiwan[1]; Department of Pathology, Keck School of Medicine, University of Southern California, Los Angeles, CA[2]; Institute of Molecular Biology, Academia Sinica, Taipei, Taiwan[3]

[*]Corresponding author. Mailing address: Graduate Institute of Immunology, National Taiwan University College of Medicine, No. 1 Jen-Ai Road, Section 1, Taipei 10051, Taiwan, Republic of China. Phone: 886 2 23217510. Fax: 886 2

23217921. E-mail: wuhsiehb@ha.mc.ntu.edu.tw.

Abstract: 248 words

Text: 7356 words

ABSTRACT

Hemorrhage is a common clinical manifestation in dengue patients. However, the pathogenic mechanism of dengue virus-induced hemorrhage awaits clarification. We established a dengue hemorrhage mouse model in immunocompetent C57BL/6 mice by injecting DV serotype 2 strain 16681 intradermally. While inoculation of 3×10^9 PFU of DV induced systemic hemorrhage in all of the mice by day 3 of infection, 1/3 of those injected with 4-8 $\times$ 10^7 PFU developed hemorrhage in the subcutaneous tissues. The mice that were inoculated with 4-8 $\times$ 10^7 PFU but did not develop hemorrhage were used as a basis for comparison to explore the pathogenic mechanism of dengue hemorrhage. The results showed that mice with severe thrombocytopenia manifested signs of vascular leakage and hemorrhage. We observed high viral titer, macrophage infiltration and TNF-α production in the local tissues are three important events that lead to hemorrhage. Immunofluorescence staining revealed that DV targeted both endothelial cells and macrophages. In addition, production of high TNF-α in tissues correlated with endothelial cell apoptosis and hemorrhage. Comparing TNF-$\alpha^{-/-}$ to $IgH^{-/-}$, $C5^{-/-}$ and wild type mice, we found that TNF-α was important to the development of hemorrhage. *In vitro* studies showed that mouse primary microvascular endothelial cells were susceptible to DV but TNF-α enhanced DV-induced apoptosis. Our mouse model illustrated that intradermal inoculation of

high titer of DV predisposes endothelial cells susceptible to TNF-α-induced cell death which leads to endothelium damage and hemorrhage development. This finding highlights the contribution of innate immune response to dengue hemorrhage.

INTRODUCTION

Dengue is a mosquito-borne viral disease that affects humans in both the tropics and subtropics. The mild form of dengue is dengue fever (DF). Approximately one-third of DF patients may have hemorrhage manifestations - ranging from mild skin hemorrhage, gingival or nasal bleeding, and gastrointestinal bleeding, to severe hemorrhage (9). Severe hemorrhage with low platelet counts, plasma leakage and pleural or other effusions is the characteristics of dengue hemorrhagic fever (DHF) (9). Therefore, hemorrhage, mild or severe, is clinically significant to dengue virus infection.

Virulent virus strains and pre-existing non-neutralizing heterologous anti-dengue antibody are reported to be the risk factors for DHF (10, 22). Immune responses involving activation of T lymphocytes, production of cytokines or chemokines and complement activation are also considered important in the pathogenesis of DHF (8, 19, 23). Higher levels of TNF-α also correlate with severe disease (2, 8). Production of TNF-α instead of IFN-γ by activated T cells is suggested to contribute to the pathogenesis of dengue (20, 21, 23). Patients with DHF have subnormal levels of C3, C4 and C5 in the serum and increased complement metabolism (26). From these studies it appears that both innate as well as adaptive immunity are implicated in severe disease. However, the key factor(s) that induces dengue hemorrhage has not

been revealed.

Over the past decade, the study of direct and indirect interactions between endothelial cells (EC) and DV has become a central focus in the understanding of the pathogenesis of dengue hemorrhage. Dengue virus (DV) antigens are detected in vascular endothelium in biopsy tissues from DHF/DSS patients, indicating DV targets endothelial cells *in vivo* (15). It remains to be clarified, however, whether dengue virus, host immune response or the complex interplay between the virus and the host causes EC damage in the infected host. An animal model will be best for the investigation of the complex relationship between DV and the host that results in hemorrhage.

Small animal models that have been used to study dengue include hu-PBL-SCID, SCID-K562, SCID-HepG2, STAT-$1^{-/-}$, AG129 with IFN-α/β and γ receptor deficiency, and immunocompetent BALB/c, A/J and C57BL/6 mice (4, 14, 16, 18, 28, 32). By intravenous, intraperitoneal or intracerebral inoculation of DV, the animals had liver pathology, thrombocytopenia, or neurological symptoms. Hemorrhage manifestation has not been reported as a prominent feature in any of these animal models.

In this study, we successfully developed a dengue hemorrhage mouse model. Immunocompetent mice receiving intradermal inoculations of DV developed hemorrhage. High viral titer, macrophage infiltration and production of TNF-α

correlated with endothelial cell apoptosis and hemorrhage. Moreover, results of gene knockout experiments clearly demonstrated that TNF-α was key to the development of hemorrhage. *In vitro* studies employing primary mouse microvascular endothelial cells demonstrated that TNF-α enhanced DV-induced apoptosis. Together these results demonstrate that dengue virus predisposes endothelial cells to TNF-α-induced apoptosis which leads to hemorrhage.

MATERIALS AND METHODS

Mice. C57BL/6, IgH$^{-/-}$ (*Igh-J*$^{tm/Cgn}$), TNF-α$^{-/-}$ (*Tnf*$^{tm/Gk1}$), A/HeJ (*Hc*^{0}) and A/J mice were originally obtained from the Jackson Laboratory (Bar Harbor, ME) and bred at the Laboratory Animal Center of National Taiwan University College of Medicine. All mice were housed in sterile cages fitted with filtered cage tops and fed with sterilized food and water. Four to five-week-old mice were used for all experiments.

Virus. Dengue virus serotype–2 (DV-2) strain 16681 was used throughout this study. DV-2 16681 was originally isolated from a Thai patient who suffered DHF (24). The virus was propagated in insect cell line C6/36 cultured in DMEM (Invitrogen, Grand Island, NY) containing 2% heat-inactivated fetal calf serum (Biological Industries, Kibbutz Beit Haemek, Israel) at 28^{o}C. Culture supernatants were collected 5 days after virus infection. The virus titer was then determined by plaque assay on BHK cell line. To prepare high titer of DV, virus supernatant was concentrated on Centriplus (10 kDa cut off, Amicon, Milipore) by centrifugation before plaque assay. The virus titer could reach 10^{10} PFU/ml after concentration. Inoculum was prepared by diluting virus stocks in PBS immediately before inoculation. To inactivate the virus, virus stocks were treated with UV at 50 mJ/cm^2 for 3 min in the SPECTROLINKER XL-1000 CROSSLINKER (Spectronics Corporation, Westbury, NY). Loss of infectivity was confirmed by plaque assay. Japanese encephalitis virus (JEV, strain

B1PS3) was also propagated in C6/36 cell line following the same protocol as that for DV.

Intradermal Infection. Mice at 4-5 weeks of age were inoculated with DV (in 0.4ml) intradermally at 4 sites on the upper back. Mice given PBS, mock C6/36 culture supernatant (Mock), equivalent titer of UV-inactivated DV (UV-DV), or viable JEV through the same route were used as controls. Western blot analysis for E and PreM proteins showed that at the same PFU (4×10^7) JEV expressed slightly higher levels of antigens than DV (data not shown). To observe hemorrhage development, mice were killed at day 3 after inoculation and the subcutaneous tissues in the back, the abdomen, and the axillary areas and thorax were exposed.

Platelet counts. Blood was collected from mice at different time points after virus inoculation and placed into an EDTA-coated Microtainer tube and mixed immediately (Becton Dickinson Vacutainer System, Franklin Lakes, NJ). Blood smear was made and read to ensure the absence of star-shape fibrin. Platelets were enumerated in Abbott Cell-Dyn 3700 (Abbott Laboratories, Abbott Park, IL) through service provided by the National Mouse Mutagenesis Program Core Facility (Acadmia Sinica, Taiwan).

RT real-time PCR and real-time RT-PCR to quantify dengue virus in mouse. To perform RT real-time PCR, tissues were collected from mice intradermally

inoculated with PBS or DV at different time points after inoculation. Cellular RNA was extracted from spleen, liver, brain, skin and subcutaneous tissue with TRIzol reagent (Invitrogen) and 3 μg of RNA was reversely transcribed to cDNA by superscript II reverse transcriptase (Invitrogen). cDNA was amplified in 25 μl reaction mixture containing primers, SYBR® Green I (Invitrogen), Flu A (Bio-Rad), and hot-start *Taq*DNA polymerase (Invitrogen) by iCycler Real-time PCR Detection System (Bio-Rad, Hercules, CA). The condition of amplification was reaction at 95℃ for 3 min, followed by 40 cycles of 95℃ for 30 sec, 56℃ for 30 sec, 72℃ for 10 sec, and 83℃ for 10 sec, then 1 cycle of 95℃ for 1 min, 57℃ for 1 min, 55℃ for 10 sec. The reaction was stopped at 10℃. Viral capsid gene was normalized against β-actin. The primers for viral capsid gene amplification were C22A and C63B as described previously (4).

Real-time RT-PCR assay was performed to quantify DV copy number in the sera (30). Briefly, RNA was extracted from mouse serum. Serial 10-fold dilution of 1×10^8 copies of positive-sense viral capsid gene were used as standards. Primers (d2C16A and d2C46B), the TaqMan TARMA probe and one-step RT-PCR master mix reagent kit (PE Biosystems, Foster City, CA) were used. The amplification condition has been published (30). The ABI Prism 7700 sequence detector (Applied Biosystems, Foster city, CA) was used to analyze the emitted fluorescence during amplification. The

sensitivity of the assay is 2.5 copies of RNA (corresponding to 357 copies per ml of serum) per reaction.

RT real-time RT-PCR to quantify TNF-α mRNA. Total cellular RNA was extracted from subcutaneous tissues and reversely transcribed to cDNA. TNF-α gene was amplified in iCycler Real-time PCR Detection System as described above. The level of TNF-α mRNA expression was normalized against β-actin. The sequences of TNF-α primers were 5'-ATCCGCGACCTCGCCCTG-3' and 5'-ACCGCCTGGAGTTCTGGAA-3'; and of β-actin primers: 5'-AGGTGTGCACCTTTTATTGGTCTCAA-3' and 5'-TGTATGAAGGTTTGGTCTCCCT-3'.

TNF-α ELISA. Subcutaneous tissues (110-114 mg) from DV-infected or control mice were harvested and homogenized in 1 ml PBS buffer by POLYTRON® (KINEMATICA® AG, Lucerne, Switzerland). Supernatants were collected from homogenized tissues after centrifugation and stored at -70℃. Culture supernatants collected from viable DV-infected, UV-DV-treated peritoneal macrophages or macrophage cultures without any treatment were also stored at -70℃. The concentration of TNF-α in tissue homogenates and culture supernatants was quantified by TNF-α ELISA (eBioscience, La. Jolla, CA). Known concentrations of recombinant murine TNF-α were used as standards.

H & E staining. Subcutaneous tissues were fixed in 4% neutral formalin solution, embedded in paraffin, and sectioned at 3 μm thickness. After deparaffinization and rehydration, the sections were stained with hematoxylin and eosin. The sections were then dehydrated before mounting.

Immunofluorescence staining. Subcutaneous tissues removed from control as well as mice inoculated intradermally with viable DV or UV-DV were embedded in O.C.T. in dry ice bath. Frozen tissues were then cryosectioned (Shandon, CRYOTOME® SME, Pittsburgh, PA) in 10-15 μm thickness. The sections were fixed in acetone for 5 min then blocked by treating with PBS containing 5% goat serum. PE-conjugated rat anti-mouse Mac-1 Ab (clone M1/70), PE-conjugated rat anti-mouse TNF-α Ab (clone MP6-XT22), PE-conjugated rat anti-mouse CD31 Ab (clone PECAM-1) or FITC-conjugated rat anti-mouse F4/80 Ab (clone BM8) was added. It has been confirmed that Mac-1^+ cells in subcutaneous tissues were F4/80^+, $CD14^+$ (clone Sa2-8) and $CD207^-$ (clone eBio RMUL.2) macrophages. To double stain macrophage and TNF-α, FITC-conjugated anti-F4/80 and PE-conjugated anti-TNF-α Abs were added simultaneously on the same cryosection. Hoechst 33258 (Sigma-Aldrich) was used to stain nuclei. All antibodies for immunofluorescence staining were obtained from eBioscience.

In situ detection of DNA fragmentation. Tissue cryosections or cell monolayers

were fixed in 4 % paraformaldehyde at room temperature for 10 min then treated with 3% H_2O_2 in methanol. Cryosections or monolayers were permeabilized with 0.1 % Triton®X-100 in 0.1 % sodium citrate on ice for 2 min. To detect apoptotic cells in tissues, FITC-conjugated TdT-mediated dUTP nick end labeling mixture (*In Situ* Cell Death Detection Kit, Roche Applied Science, Indianapolis IN) were added onto tissue sections. PE-conjugated anti-Mac-1 or PE-conjugated anti-CD31 Ab was then used to further determine the type of cells undergoing apoptosis. To detect cell death in primary EC monolayer, converter-POD (peroxidase-conjugated anti-fluorescein antibody) was added and DAB was used as substrate for color development. Hoechst 33258 was used to stain nuclei.

Staining for dengue viral antigen. Cryosections were fixed with 4 % paraformaldehyde at room temperature for 10 min. To detect viral Ag on cryosection, polyclonal rabbit anti-DV antiserum was added and the sections were left at 4℃ overnight. PE-conjugated anti-rabbit Ab (Invitrogen) was then added to the sections and left at 4℃ for 1h. To detect DV target cells, PE-conjugated anti-Mac-1 or PE-conjugated anti-CD31 Ab and rabbit anti-DV Ab were added to the same section simultaneously. After incubation at 4℃ overnight, FITC-conjugated anti-rabbit Ab was added. To determine whether DV Ag-expressing cells were apoptotic, tissue sections were double stained with FITC-conjugated TdT-mediated dUTP nick end

labeling mixture and rabbit anti-DV Ab following the same protocol.

Mouse microvascular endothelial cell isolation. The method of isolation of mouse microvascular endothelial cells (ECs) was adopted from a previous publication (33). Briefly, brains from mice at 8-12 weeks of age were collected. Cerebral cortices were harvested and the solid tissues were homogenized in RPMI medium containing 2% inactivated FCS by glass tissue grinder. The homogenates were separated by 15% dextran (average molecular weight 68,800 Da, Sigma-Aldrich) and treated with colleagenase/dispase mixture (Boehringer Mannheim, Indianapolie, IN) at 0.05% (weight/volume) at 37℃ for 6 h with occasional agitation. Cells were washed with buffer and resuspended in RPMI medium containing 30 μg/ml ENDO-GRO (Sigma-Adrich). ECs were grown in flasks pre-coated with 1% gelatin. Cells at passages 3-4 containing 90-95% $CD31^+$ cells were used in all experiments.

Dengue virus infection of cells. Thioglycolate-elicited peritoneal macrophages or ECs were seeded onto 12 mm round glass cover-slips (Assistant, Sondheim, Germany). The cells were cultured in RPMI medium containing 1% inactivated FCS at 37℃ for 2h. Viable DV or UV-DV was then added to the monolayers at MOI of 5 or 10 and incubated at 37℃ for 2h with gentle shaking every 15 min. The monolayer was washed with HBSS and cultured in respective fresh growth medium. Culture supernatants from infected macrophage monolayers were harvested after infection and

stored at -70℃ before assay. Undiluted supernatants were used to asses the effect of DV-infected macrophage culture supernatants on EC. The percentage of apoptotic cells was determined by *In Situ* Cell Detection System as described above. To neutralize the effect of TNF-α, supernatants from DV-infected macrophages were pre-incubated with neutralizing anti-mouse TNF-α antibody (clone MP6-XT3, eBioscience) before addition to the endothelial cell culture. To assay the effect of TNF-α, EC with or without DV infection was cultured in medium containing human recombinant TNF-α (hu-rTNF-α, Biosource, Camarillo, CA) at 30, 300, or 3000 pg/ml.

Statistical analysis. The SPSS (Statistical Package for the Social Sciences, SPSS Inc.) program was employed for statistical analysis. Difference between the means of experimental groups was analyzed using ANOVA and Tukey post-hoc test. Statistical significance was determined at $p<0.01$ and $p<0.05$..

RESULTS

Dengue virus induces hemorrhage in C57BL/6 mice. To mimic natural infection in humans, immunocompetent C57BL/6 mice were injected intradermally with DV. Hemorrhage developed at different sites including the subcutaneous tissue, abdomen, the intestine (Fig. 1A), the skin and lymph nodes (data not shown) at day 3 after virus inoculation. The incidence, severity and the site of hemorrhage development correlated with the size of virus inoculum. While 100% and 73% of the mice receiving 3×10^9 and 1×10^9 PFU, respectively developed systemic hemorrhage, 33% of those given 8×10^7 PFU exhibited hemorrhage at the subcutaneous tissue (Table 1, Fig. 1A and B). Notably, subcutaneous hemorrhage developed at approximately the diagonal crossing of the lines connecting the 4 injection sites and the degree of hemorrhage ranged from mild to severe (Fig. 1A and B). Interestingly, although mice exhibited severe hemorrhage after receiving high viral inoculum (Fig. 1A) they appeared healthy and no sign of paralysis was observed. To confirm that hemorrhage is DV-specific, mice inoculated with PBS, UV-inactivated DV (3×10^9 and 4×10^7 PFU), mock C6/36 supernatant, and viable JEV (4×10^7 PFU) were examined for hemorrhage development. Data showed that only the mice that were inoculated with viable DV but not any other inoculum developed hemorrhage, indicating hemorrhage development is viable DV-specific. Moreover, microscopic examination of the

subcutaneous hemorrhage tissues revealed red blood cell extravasation (Fig. 1C). These results demonstrate that intradermal inoculation of DV induces hemorrhage in mice and hemorrhage is accompanied by vascular leakage.

Severe thrombocytopenia is associated with hemorrhage. Next, we collected peripheral blood from mice receiving 4×10^7 PFU of DV and tested whether thrombocytopenia is associated with hemorrhage. Since about 2/3 of mice receiving 4×10^7 PFU did not develop hemorrhage, they were used as non-hemorrhage (nH) controls. At day 3 after inoculation, the platelet counts in mice injected with DV were significantly lower ($p<0.01$) in both hemorrhagic (H, $732.2 \pm 109.5 \times 10^{-3}/\mu l$) and non-hemorrhagic ($772.7 \pm 49.9 \times 10^{-3}/\mu l$) mice than in control mice ($923.3 \pm 73.35 \times 10^{-3}/\mu l$). At day 7, the counts in nH mice ($772.5 \pm 36.5 \times 10^{-3}/\mu l$) remained at the same level as day 3, but that in H mice ($578.0 \pm 71.9 \times 10^{-3}/\mu l$) were further reduced ($p<0.05$). These data demonstrate that DV infection induces thrombocytopenia and severe thrombocytopenia is associated with hemorrhage.

Dengue virus distribution in mice after intradermal inoculation. To study the relationship between virus titer and hemorrhage, we compared virus capsid gene expression in tissues from H and nH mice. At day 3 after virus inoculation viral capsid gene was detectable in spleen, liver, brain, skin and serum in both H and nH mice but the level of expression was significantly higher in H than in nH mice (Fig. 2A and B).

Although viral capsid RNA was no longer detectable in the subcutaneous tissues at day 3 after inoculation, it was expressed at day 1 (Fig. 2A), showing that DV was present in subcutaneous tissues soon after intradermal inoculation but was cleared thereafter. Furthermore, while viral capsid gene copy number increased from day 1 to 3 in the serum of H and nH mice, it was significantly higher in H than in nH mice (Fig. 2B). Immunofluorescence staining also showed the presence of viral antigen in the skin (increased from day 1 to 3, Fig. 2C) and subcutaneous tissues (at day 1, Fig. 2D) after inoculation. Together these data indicate a strong correlation between high viral titer and hemorrhage development.

Macrophages infiltrate and produce TNF-α in the hemorrhage tissue. To investigate the contribution of immune cells to hemorrhage development, subcutaneous tissues from H and nH mice were examined for the presence of NK cells, neutrophils, macrophages, dentritic cells and T cells. The results revealed no appreciable numbers of NK ($NK1.1^+$), T ($CD3^+$) cells, dendritic cells ($CD11c^+$), Langerhans cells ($CD207^+$) or neutrophils ($Gr.1^+$) were present (data not shown). Only macrophages ($Mac\text{-}1^+/F4/80^+/ CD14^+$) were detected in the subcutaneous tissues of both H and nH mice, but it was 2-fold higher ($p<0.05$) in H mice (21.5 ± 4.2%) than in nH mice (10.6 ± 2.0%) (Fig. 3).

Since it has been reported that high TNF-α expression correlates with hemorrhage

(12), *in situ* TNF-α expression in subcutaneous tissues was then quantified. RT real-time PCR results show a significant increase of TNF-α mRNA in H mice over the PBS control at day 3 after DV infection (Table 2). It was further increased in H but not in nH mice at day 3 (Table 2). Quantitation of *in situ* TNF-α protein in tissue homogenates show that while TNF-α levels increased from day 1 on, that in H mice (155.2 ± 65.7 pg/ml) was about 8 times of that in nH mice (19.2 ± 1.1 pg/ml) at day 3 after infection (Table 2). These results indicate a strong association between macrophage infiltration, TNF-α production and hemorrhage.

Immunofluorescence staining of subcutaneous hemorrhage tissues showed that TNF-α colocalized with macrophages (Fig. 4A), indicating that macrophages are a likely source of TNF-α. *In vitro* experiments were performed to determine whether DV-infected macrophages produce TNF-α. Fig. 4B shows that DV induced macrophage production of TNF-α at as early as 6h (122.1 ± 32.8 pg/ml) after infection. The level of TNF-α reached the peak at 12h (329.0 ± 86.2 pg/ml) and declined thereafter. These results together revealed that macrophage infiltration and production of TNF-α in the tissues after DV infection are two important events that lead to hemorrhage.

TNF-α is key to development of dengue hemorrhage in mice. TNF-α $^{-/-}$ mice were employed to ascertain the role of TNF-α in hemorrhage development. Since

antibody and complement have been implicated in the protection as well as the pathogenesis of hemorrhage in dengue (23) and DV infection induced DV-specific IgM and IgG production and C3 deposition were observed in hemorrhage tissues (data not shown), mice with IgH and complement defects were used as control. Table 3 shows that the percentages of TNF-$\alpha^{-/-}$ mice (5%) that developed hemorrhage was significantly lower (p<0.05) than the wild type, $IgH^{-/-}$ and A/HeJ ($C5^{-/-}$) mice. The percentage of hemorrhage development in $IgH^{-/-}$ (29%) and $C5^{-/-}$ (38%) mice were not much different from their respective wild type mice (35% and 33%, respectively). These data clearly indicate that TNF-α, but not antibody production or complement deposition, is key to the development of hemorrhage in DV-infected mice.

ECs are targets of dengue virus and become apoptotic in the hemorrhage tissue. To determine whether hemorrhage is accompanied by cell death, subcutaneous tissues were stained by TUNEL reagents. The results show an overwhelming presence of apoptotic cells in tissues from H (37.2 ± 18.0 %) but not nH (1.0 ± 0.4 %) mice at day 3 after infection (p<0.05). Double-staining revealed that apoptotic cells were DV Ag^{+} (Fig. 5). Further analysis of the type of cells undergoing apoptosis revealed as high as 94.0% of $CD31^{+}$ ECs (1) and only 23% of macrophages ($F4/80^{+}$/$Mac\text{-}1^{+}$) in the hemorrhage tissues were apoptotic, indicating a strong link between endothelial cell apoptosis and hemorrhage. In addition, double-staining unveiled that both ECs

and macrophages are targets for DV at the early phase of infection (Fig. 6).

In vitro experiments demonstrate TNF-α in the DV-infected macrophage culture supernatant induces EC apoptosis. Primary microvascular ECs were isolated to study their susceptibility to DV- and TNF-α-induced cell death. The results demonstrate that DV alone at MOI of 5 and 10, induced 11.0 ± 1.1% and 29.9 ± 5.6% EC apoptosis, respectively, at 24 h of infection (Fig. 7A). Recombinant TNF-α at 3000 pg/ml but not at 30 or 300 pg/ml induced EC death (Fig. 7A). Interestingly, addition of 300 pg/ml of TNF-α to DV-infected cells increased cell death from 11.0 ± 1.1% to 21.0 ± 3.8% ($p<0.01$) at MOI of 5 and from 29.9 ± 5.6% to almost 3-fold to as high as 85.4 ± 8.3% ($p<0.05$) at MOI of 10, and addition of 3000 pg/ml of TNF-α increased cell death to 92.0 ± 0.3% at MOI of 10. It is worth noting that addition of 300 pg/ml of TNF-α to UV-DV-treated cells did not increase the percentage of cell death compared to TNF-α-treated uninfected cells, indicating EC death is not a result of over-stimulation by high concentration of antigen.

Moreover, treatment with 12h-supernatants from DV-infected macrophage cultures completely destroyed EC monolayers pre-infected with DV (Fig. 7B). Over 95% of DV-infected ECs at MOI of 10 were apoptotic after treatment with 12h-supernatants (Fig. 7C). Importantly, the effect of macrophage culture supernatants on ECs was completely neutralized by anti-TNF-α-antibody pretreatment, regardless the virus titer

1 the ECs were infected with (Fig. 7B and C). These results together demonstrate that
2 DV induces macrophage production of TNF-α and TNF-α enhances DV-induced EC
3 death.

DISCUSSION

It has been documented that high level of TNF-α is associated with severe dengue disease (2, 13, 34). There is also a positive relationship between soluble TNFR (sTNFR)/sTNFR II levels and the severity of DHF (2, 12). Single-nucleotide polymorphism analysis identified TNF-α polymorphism at TNF-308A allele to be a possible risk factor for hemorrhagic manifestations in DF patients (6). TNF-α promoter with polymorphism at position -308 is a stronger transcriptional activator which is responsible for production of higher levels of TNF-α (31). The TNF-308A-positive patients are more likely to develop DHF than TNF-308A-negative patients (6). These observations together strongly indicate that high TNF-α is critical in the pathogenesis of severe dengue illness. However, the direct causal relationship between TNF-α and dengue hemorrhage has not been clearly established. We showed in this study the direct relationship between *in situ* high levels of TNF-α and hemorrhage in a DV-infected host (Table 2) and that without TNF-α, the chances to develop hemorrhage are greatly diminished (Table 3). In addition, we observed that tissue viral titer in $TNF^{-/-}$ mice was higher than in wild type mice, yet mice did not develop hemorrhage (data not shown). These data together provide direct evidence for the critical role of TNF-α in dengue hemorrhage.

Our results demonstrated that DV infection induces mouse macrophage to produce

TNF-α (Fig. 4A and B). It has been reported that human monocytes infected by DV produce TNF-α (3, 5). Sensitized T cells from dengue patients also produce TNF-α in culture upon restimulation (7, 20). A recent publication reported the cytokine responses of DV-specific memory $CD4^+$ T cells in PBMC of volunteers who received experimental live attenuated monovalent dengue vaccines (21). While antigens from homotypic DV elicit the highest IFN-γ response, peptide sequences from heterotypic DV elicits $CD4^+$ T cell responses with higher TNF-α^+ to IFN-γ^+ T cell ratios. In our mouse model, hemorrhage develops at as early as day 3 after virus inoculation, a time too early for T cells to mount a significant response. Thus, our model illustrates the importance of innate immune response to DV infection in the pathogenesis of hemorrhage. However, it is entirely possible that inappropriate T cell activation resulting in the production of TNF-α in later stage of primary infection or in secondary infection may worsen the disease.

Vascular ECs line the inner surface of blood vessels and play an important role in vascular functions (17). It is thus a logical assumption that hemorrhage or altered vascular permeability is a result of EC damage. Whether DV targets ECs in dengue patients has been a point of debate for decades until recently Jessie et al. reported their immunohistochemical staining and *in situ* hybridization of biopsy and autopsy specimens from DF/DHF/DSS patients (15). Their report clearly showed the presence

of dengue viral antigens in sinusoidal ECs of the liver as well as in the vascular endothelium of the lung (15). Our study of the hemorrhage mouse tissue also showed that DV targets ECs (Fig. 6). Double-staining of hemorrhage tissues with anti-NS1 and anti-CD31 or anti-CD14 antibodies revealed that viral NS1 antigen was detectable in $CD31^+$ cells at 6 h, and the intensity increased at 12 h and 24 h after inoculation, but not in $CD14^+$ cells at any early of these early time points, confirming that DV replicates in endothelial cells soon after infection. In addition, unlike what was observed in human skin, neither $CD11c^+$ nor $CD207^+$ cells stained for DV Ag at these early time points (data not shown). Thus, it appears that DC does not have major contribution to dengue hemorrhage in our mouse model and EC as an early target of DV is predisposed by DV to the deleterious events that occur subsequently.

The loss of endothelium integrity in DHF/DSS has long been attributed to the inflammatory mediators released by mononuclear phagocytes of which TNF-α is the primary candidate (10, 11). However, macrophage production of TNF-α is common to a variety of infections (29) in which profound alteration of endothelium permeability may not be a prominent feature. It remains a question why TNF-α is specifically of importance to dengue hemorrhage. In their report showing a positive relationship between high sTNFR levels and disease severity, Bethell et al. proposed that the effect of systemic cytokines on endothelium is determined by the local events

occur, such as viral infection (2). It is interesting to note that no viral RNA was detectable at day 3 when hemorrhage develops at the subcutaneous tissues although the presence of virus was documented at day 1 (Fig. 2A). Thus, it appears that the presence of DV predisposes the endothelium to vascular damage triggered by TNF-α, yet its concurrent presence is not required for hemorrhage development.

Nonhuman primates have been used to study dengue (9). The animals showed no signs of disease but developed viremia. The dengue hemorrhage mouse model we reported in this study does not show all the characteristics of a natural DV infection in humans but the mice develop hemorrhage and thrombocytopenia. After a person is bitten by an infective mosquito, the virus undergoes replication and circulates in the peripheral blood during the incubation period of 3 to 14 days (average, 4 to 7 days) before fever onset (25). Introducing high titers of DV through 4 intradermal inoculations was critical to the success of our hemorrhage model. The virus introduced intradermally, mimicking the natural route of infection, was efficiently spread to other tissues and the circulation (Fig. 2A and B) and hemorrhage developed within only 3 days. It appears introducing high DV inoculum intradermally quickly meets the threshold of virus titer that is required to stage a pathogenic event in the murine host. Therefore, our mouse model only models the immediate events that lead to hemorrhage, but not the entirety of the pathogenesis of human dengue hemorrhage.

It is noteworthy that hemorrhage development is DV-specific and virus viability is essential. Introducing neither UV-DV nor viable JEV, another mosquito-borne flavivirus, through the same route at otherwise equivalent titer did not result in hemorrhage. In addition, injecting recombinant TNF-α (8μg) along with mock C6/36 supernatants through the same route did not induce hemorrhage (data not shown), excluding the possibility that injury (as might be induced through needle sticks) is involved in the process. Based on these observations we speculate that specific interaction between DV and cells, especially at high DV titer, perhaps through the activity of a specific viral component(s), is critical to the development of hemorrhage.

In the present study, we established a dengue hemorrhage mouse model through intradermal inoculation of high titer of virus. Employing this mouse model we identified TNF-α as one of the key host factors in causing dengue hemorrhage, which is consistent with the recent observation reported by Shresta et al that TNF-α is the key mediator of severe DV-induced disease in mice (27). In our model, hemorrhage develops within 3 days after virus inoculation, a time too early for adaptive immune response to take effect. Although our finding emphasizes the importance of innate immune response in hemorrhage development, it does not rule out the contribution of non-neutralizing antibody-dependent enhancement in increasing infection or the involvement of TNF-α producing activated T cells in the pathogenesis of dengue

hemorrhage in secondary infection. Experiments are currently undertaken to address these questions.

Acknowledgments

This work was supported by funds from the National Research Program for Genomic Medicine (grant NSC 95-3112-B-002-027), National Health Research Institutes (grant NHRI-CN-CL9302P) of the Republic of China and the National Taiwan University Hospital (grant NTUH 95A21-2).

We thank Dr. Chwan-Chuen King for her helpful discussions. We also thank National Mouse Mutagenesis Program Core Facility (Academia Sinica, Taiwan) for processing blood samples.

REFERENCES

1. **Baldwin, H. S., H. M. Shen, H. C. Yan, H. M. DeLisser, A. Chung, C. Mickanin, T. Trask, N. E. Kirschbaum, P. J. Newman, S. M. Albelda, and et al.** 1994. Platelet endothelial cell adhesion molecule-1 (PECAM-1/CD31): alternatively spliced, functionally distinct isoforms expressed during mammalian cardiovascular development. Development **120:**2539-2553.
2. **Bethell, D. B., K. Flobbe, X. T. Cao, N. P. Day, T. P. Pham, W. A. Buurman, M. J. Cardosa, N. J. White, and D. Kwiatkowski.** 1998. Pathophysiologic and prognostic role of cytokines in dengue hemorrhagic fever. J. Infect. Dis. **177:**778-782.
3. **Carr, J. M., H. Hocking, K. Bunting, P. J. Wright, A. Davidson, J. Gamble, C. J. Burrell, and P. Li.** 2003. Supernatants from dengue virus type-2 infected macrophages induce permeability changes in endothelial cell monolayers. J. Med. Virol. **69:**521-528.
4. **Chen, H. C., S. Y. Lai, J. M. Sung, S. H. Lee, Y. C. Lin, W. K. Wang, Y. C. Chen, C. L. Kao, C. C. King, and B. A. Wu-Hsieh.** 2004. Lymphocyte activation and hepatic cellular infiltration in immunocompetent mice infected by dengue virus. J. Med. Virol. **73:**419-431.
5. **Espina, L. M., N. J. Valero, J. M. Hernandez, and J. A. Mosquera.** 2003. Increased apoptosis and expression of tumor necrosis factor-alpha caused by infection of cultured human monocytes with dengue virus. Am. J. Trop. Med. Hyg. **68:**48-53.
6. **Fernandez-Mestre, M. T., K. Gendzekhadze, P. Rivas-Vetencourt, and Z. Layrisse.** 2004. TNF-alpha-308A allele, a possible severity risk factor of hemorrhagic manifestation in dengue fever patients. Tissue Antigens

64:469-472.

7. **Gagnon, S. J., F. A. Ennis, and A. L. Rothman.** 1999. Bystander target cell lysis and cytokine production by dengue virus-specific human CD4(+) cytotoxic T-lymphocyte clones. J. Virol. **73:**3623-3629.

8. **Green, S., D. W. Vaughn, S. Kalayanarooj, S. Nimmannitya, S. Suntayakorn, A. Nisalak, R. Lew, B. L. Innis, I. Kurane, A. L. Rothman, and F. A. Ennis.** 1999. Early immune activation in acute dengue illness is related to development of plasma leakage and disease severity. J. Infect. Dis. **179:**755-762.

9. **Gubler, D. J.** 1998. Dengue and dengue hemorrhagic fever. Clin. Microbiol. Rev. **11:**480-496.

10. **Halstead, S. B.** 1989. Antibody, macrophages, dengue virus infection, shock, and hemorrhage: a pathogenetic cascade. Rev. Infect. Dis. **11 Suppl 4:**S830-839.

11. **Halstead, S. B.** 2002. Dengue. Curr. Opin. Infect. Dis. **15:**471-476.

12. **Hober, D., A. S. Delannoy, S. Benyoucef, D. De Groote, and P. Wattre.** 1996. High levels of sTNFR p75 and TNF alpha in dengue-infected patients. Microbiol. Immunol. **40:**569-573.

13. **Hober, D., L. Poli, B. Roblin, P. Gestas, E. Chungue, G. Granic, P. Imbert, J. L. Pecarere, R. Vergez-Pascal, P. Wattre, and et al.** 1993. Serum levels of tumor necrosis factor-alpha (TNF-alpha), interleukin-6 (IL-6), and interleukin-1 beta (IL-1 beta) in dengue-infected patients. Am. J. Trop. Med. Hyg. **48:**324-331.

14. **Huang, K. J., S. Y. Li, S. C. Chen, H. S. Liu, Y. S. Lin, T. M. Yeh, C. C. Liu, and H. Y. Lei.** 2000. Manifestation of thrombocytopenia in dengue-2-virus-infected mice. J. Gen. Virol. **81:**2177-2182.

15. **Jessie, K., M. Y. Fong, S. Devi, S. K. Lam, and K. T. Wong.** 2004. Localization of dengue virus in naturally infected human tissues, by immunohistochemistry and in situ hybridization. J. Infect. Dis. **189:**1411-1418.

16. **Johnson, A. J., and J. T. Roehrig.** 1999. New mouse model for dengue virus vaccine testing. J. Virol. **73:**783-786.

17. **Kaiser, L., and H. V. Sparks, Jr.** 1987. Endothelial cells. Not just a cellophane wrapper. Arch. Intern. Med. **147:**569-573.

18. **Lin, Y. L., C. L. Liao, L. K. Chen, C. T. Yeh, C. I. Liu, S. H. Ma, Y. Y. Huang, Y. L. Huang, C. L. Kao, and C. C. King.** 1998. Study of Dengue virus infection in SCID mice engrafted with human K562 cells. J. Virol. **72:**9729-9737.

19. **Malasit, P.** 1987. Complement and dengue haemorrhagic fever/shock syndrome. Southeast Asian J. Trop. Med. Public Health **18:**316-320.

20. **Mangada, M. M., T. P. Endy, A. Nisalak, S. Chunsuttiwat, D. W. Vaughn, D. H. Libraty, S. Green, F. A. Ennis, and A. L. Rothman.** 2002. Dengue-specific T cell responses in peripheral blood mononuclear cells obtained prior to secondary dengue virus infections in Thai schoolchildren. J. Infect. Dis. **185:**1697-1703.

21. **Mangada, M. M., and A. L. Rothman.** 2005. Altered cytokine responses of dengue-specific CD4+ T cells to heterologous serotypes. J. Immunol. **175:**2676-2683.

22. **Rico-Hesse, R.** 1990. Molecular evolution and distribution of dengue viruses type 1 and 2 in nature. Virology **174:**479-493.

23. **Rothman, A. L., and F. A. Ennis.** 1999. Immunopathogenesis of Dengue hemorrhagic fever. Virology **257:**1-6.

24. **Russell, P. K., S. Udomsakdi, and S. B. Halstead.** 1967. Antibody response in dengue and dengue hemorrhagic fever. Jpn. J. Med. Sci. Biol. **20:**103-108.

25. **Sabin, A. B.** 1952. Research on dengue during World War II. Am. J. Trop. Med. Hyg. **1:**30-50.

26. **Shaio, M. F., F. Y. Chang, and S. C. Hou.** 1992. Complement pathway activity in serum from patients with classical dengue fever. Trans R. Soc. Trop. Med. Hyg. **86:**672-675.

27. **Shresta, S., K. L. Sharar, D. M. Prigozhin, P. R. Beatty, and E. Harris.** 2006. Murine model for dengue virus-induced lethal disease with increased vascular permeability. J. Virol. **80:**10208-10217.

28. **Shresta, S., K. L. Sharar, D. M. Prigozhin, H. M. Snider, P. R. Beatty, and E. Harris.** 2005. Critical roles for both STAT1-dependent and STAT1-independent pathways in the control of primary dengue virus infection in mice. J. Immunol. **175:**3946-3954.

29. **Vassalli, P.** 1992. The pathophysiology of tumor necrosis factors. Annu. Rev. Immunol. **10:**411-452.

30. **Wang, W. K., T. L. Sung, Y. C. Tsai, C. L. Kao, S. M. Chang, and C. C. King.** 2002. Detection of dengue virus replication in peripheral blood mononuclear cells from dengue virus type 2-infected patients by a reverse transcription-real-time PCR assay. J. Clin. Microbiol. **40:**4472-4478.

31. **Wilson, A. G., J. A. Symons, T. L. McDowell, H. O. McDevitt, and G. W. Duff.** 1997. Effects of a polymorphism in the human tumor necrosis factor alpha promoter on transcriptional activation. Proc. Natl. Acad. Sci. U S A **94:**3195-3199.

32. **Wu, S. J., C. G. Hayes, D. R. Dubois, M. G. Windheuser, Y. H. Kang, D. M. Watts, and D. G. Sieckmann.** 1995. Evaluation of the severe combined

immunodeficient (SCID) mouse as an animal model for dengue viral infection. Am. J. Trop. Med. Hyg. **52:**468-476.

33. **Wu, Z., F. M. Hofman, and B. V. Zlokovic.** 2003. A simple method for isolation and characterization of mouse brain microvascular endothelial cells. J. Neurosci. Methods. **130:**53-63.

34. **Yadav, M., K. R. Kamath, N. Iyngkaran, and M. Sinniah.** 1991. Dengue haemorrhagic fever and dengue shock syndrome: are they tumour necrosis factor-mediated disorders? FEMS Microbiol. Immunol. **4:**45-49.

TABLE 1. Correlation between virus inoculum and hemorrhage[a]

Virus titer (PFU)	No. of mice with hemorrhage/No. of mice inoculated (Percentage of mice with hemorrhage)
3×10^9	16/16 (100)[b]
1×10^9	11/15 (73)[b]
8×10^7	11/33 (33)[c]

[a]C57BL/6 mice were inoculated intradermally with indicated titer of viable DV at 4 sites on the upper back. Hemorrhage was observed at day 3 after inoculation. The data are pooled from 3 to 4 experiments.

[b]Mice developed systemic hemorrhage as shown in Fig. 1A.

[c]Mice developed hemorrhage in the subcutaneous tissue as shown in Fig. 1B.

TABLE 2. High TNF-α expression correlates with hemorrhage

TNF-α	Inoculum[c]	Days after inoculation[d] 1	2	3
mRNA (TNF-α/β-actin)[a]	Live-DV	0.43 ± 0.09	0.63 ± 0.05	(H) 1.10 ± 0.22** † (nH) 0.47 ± 0.14
	UV-DV	ND[e]	ND	0.46 ± 0.09[f]
	PBS	ND	ND	0.50 ± 0.01[f]
Protein (pg/ml)[b]	Live-DV	28.4 ± 4.5*	65.5 ± 15.2*	(H) 155.2 ± 65.7* † (nH) 19.2 ± 1.1*
	UV-DV	ND	ND	15.6 ± 1.0[f]
	PBS	ND	ND	14.1 ± 0.2[f]

[a]The relative levels of TNF-α mRNA expression were determined by RT real-time PCR.

[b]Concentration of TNF-α protein in the supernatants of tissue homogenates was quantified by ELISA.

[c]Mice were inoculated intradermally with 4×10^7 PFU of viable DV (Live-DV), UV-inactivated DV (UV-DV) or PBS on the upper back.

[d]Subcutaneous tissues were collected from mice at days 1, 2 and 3 after Live-DV, at day 3 after PBS or UV-DV inoculation. Data at each time point were pooled from 6 mice. The averages of values are expressed as mean ± SD.

[e]ND = not done

[f]No hemorrhage observed in UV-DV or PBS-inoculated mice.

* and ** indicate $p<0.01$ and $p<0.05$ compared against PBS-inoculated mice, respectively; †, $p<0.01$ compared against nH mice at day 3.

TABLE 3. TNF deficiency diminishes DV-induced hemorrhage

Mice[a]	No. of mice with hemorrhage/No. of mice inoculated (Percentage of mice with hemorrhage)[b]
C57BL/6	**7/20 (35)**
IgH$^{-/-}$	**4/14 (29)**
TNF-α$^{-/-}$	**1/20 (5)****
A/J	**6/18 (33)**
A/HeJ	**8/22 (36)**

[a]IgH$^{-/-}$, TNF-α$^{-/-}$ mice and their wild type C57BL/6 counterparts as well as A/HeJ mice and their wild type A/J counterparts were injected intradermally with 4×10^7 PFU of viable DV. The data are pooled from 3 experiments.

[b]Mice developed hemorrhage in the subcutaneous tissue as shown in Fig. 1B.

** indicates the *p* value comparing TNF-α$^{-/-}$ to wild type, IgH$^{-/-}$, A/J, or A/HeJ mice each was <0.05.

FIGURE LEGENDS

FIG. 1. Intradermal inoculation of DV induces hemorrhage in immunocompetent mice. (A) C57BL/6 mice were injected intradermally with 3×10^9 PFU of viable DV at four different sites in the back as indicated by arrows. Subcutaneous tissue, abdomen and intestine were exposed at day 3 after inoculation. (B) Mice were inoculated intradermally at 4 sites as indicated by arrows with PBS, 4-8 $\times 10^7$ PFU of viable DV (Live DV), or UV-DV. Hemorrhage was observed in subcutaneous tissues at day 3 of infection. Hemorrhage sites in the tissues are circled. (C) Sections of subcutaneous tissues from mice inoculated with PBS as well as viable DV as in (B) were stained with hematoxylin and eosin. The magnification was 100X (left) and 400X (right).

FIG. 2. DV capsid gene and antigen expression in tissues. Mice were inoculated with 4 $\times 10^7$ PFU viable DV (DV). (A) RNA was extracted from tissues collected at days 1 and 3 after virus inoculation. Viral capsid gene was amplified by RT real-time PCR. The relative levels of capsid RNA was determined as described in Materials and Methods. ** indicates $p<0.05$, comparing the mean value in H to that in nH mice. Each time points are mean value of tissues from 4 different mice. (B) Mouse serum was collected at days 1, 2 and 3 after DV inoculation. Viral capsid gene was amplified by real-time RT-PCR. Capsid gene copy number per μl of serum was determined against the standards. Hemorrhage

manifestation in each mouse was determined at day 3 after inoculation. ** indicates $p<0.05$, comparing the mean of viral copy numbers in H (soild bar) to that in nH (open bar) mice. (C) Skin and (D) subcutaneous tissues from mice inoculated with viable virus (Live-DV) or UV-DV were collected at days 1 and 3 after inoculation. DV antigen was detected by rabbit polyclonal anti-DV and PE-conjugated goat anti-rabbit Ig antibodies. The cryosections of tissues collected from H mice were stained with naïve rabbit serum as control to examine the specificity of rabbit anti-DV serum. Hoechst 33258 stain reveals the nuclei. Data presented are representative of 3 repeated experiments. The magnification was 200X (C) and 400X (D).

FIG. 3. Macrophage infiltration in hemorrhage tissue. The cryosections of subcutaneous tissues collected from mice injected with PBS, 4×10^7 PFU of viable DV (Live-DV) or equivalent titer of UV-DV at days 1 and 3 after inoculation were stained with PE-conjugated rat anti-mouse Mac-1 Ab. Cryosections of tissues from H mice were stained with PE-conjugated anti-mouse isotype IgG2b Ab as staining control. Mice with (H) or without hemorrhage (nH) were determined at day 3 after inoculation. The number ± SD on the top of each picture indicates the mean percentage of Mac-1^+ cells in each group. The percentage of Mac-1^+ cells was determined by dividing the count of Mac-1^+ cells by the total number of Hoechst$^+$ cells in the same field. The data were pooled from

counting cells in 4 sections obtained from 4 different mice. Three to 5 fields in each section and total of 750-800 cells were counted. **, $p<0.05$ comparing the number of infiltrating macrophages in tissue from H mice to that from nH mice at day 3 after infection.

FIG. 4. DV induces macrophage TNF-α production. (A) Mice were inoculated with 4×10^7 PFU of viable DV. The cryosections of subcutaneous tissues from hemorrhage mice were stained with FITC-conjugated anti-F4/80 and PE-conjugated anti-TNF-α Abs. Isotype Ab staining with controls FITC-conjugated anti-mouse IgG2a and PE-conjugated anti-mouse IgG1 were negative. Data presented are representative of 3 repeated experiments. The magnification was 400X. (B) Supernatants from DV-infected macrophages (MOI of 10) were collect at 0, 6, 12, 21 and 48 h after infection (h.p.i.). The TNF-α concentrations in the supernatants were determined by ELISA. ** indicates $p<0.05$ comparing the mean TNF-α concentration in the supernatants from DV-infected macrophages to that from macrophages cultured in medium without virus. The levels of TNF-α in supernatants from macrophages cultured in medium or medium containing UV-DV were below the level of detection (data not shown). Data presented are pooled from 3 experiments.

FIG. 5. DV antigen-expressing cells are apoptotic. The cryosection of subcutaneous

tissues collected from mice injected with 4×10^7 PFU of viable DV (Live-DV) or UV-inactivated DV (UV-DV) at day 2 after inoculation were stained with rabbit anti-DV serum plus PE-conjugated goat anti-rabbit IgG, FITC-conjugated TdT-mediated dUTP nick end labeling mixture and Hoechst 33258 stain.

FIG. 6. DV targets ECs and macrophages in the subcutaneous tissue after intradermal inoculation. The cryosections of subcutaneous tissues collected from mice receiving 4×10^7 PFU of viable DV at day 1 after inoculation were stained with (A) rabbit anti-DV antiserum plus FITC-conjugated goat anti-rabbit IgG, PE-conjugated anti-Mac-1 or (B) rabbit anti-DV antiserum plus FITC-conjugated goat anti-rabbit IgG, PE-conjugated anti-CD31 Ab and Hoechst 33258 stain.

FIG. 7. Macrophage produces TNF-α to enhance DV-induced EC death. (A) Mouse microvascular ECs were infected with viable DV at MOI of 5, 10 or cultured in medium alone. Recombinant TNF-α was added to the EC culture with (black bar) or without DV (open bar) infection. ECs treated with UV-inactivated DV (UV-DV) and rTNF-α used as control (hatched bar). Cell death was determined by TUNEL reaction. The percentage of apoptotic cells in each condition was determined by dividing the number of $TUNEL^+$ cells by the total number of $Hoechst^+$ nuclei counted. Data are pooled from 3 repeated experiments. (B) DV-infected ECs were treated with culture supernatants from

DV-infected macrophage cultures collected at 6 or 12 h after infection. Half of the macrophage culture supernatants were pretreated with neutralizing anti-TNF-α antibody at 1 μg/ml before adding to the EC monolayer. The EC monolayer morphology was observed by phase contrast light microscopy. The magnification is 200X. (C) Microvascular ECs were cultured in medium alone or infected with DV at MOI of 5 or 10 without other treatments. Other infected ECs were treated with 12-h supernatants collected from DV-infected macrophage cultures with or without anti-TNF-α Ab pretreatment. Infected ECs treated with anti-TNF-α Ab were used as controls. Isotype rat IgG1 was used to demonstrate the specificity of anti-TNF-α Ab-mediated block. Percent EC apoptosis was calculated as described under (A). Data were pooled from 3 separate experiments. * and ** indicate $p<0.01$ and $p<0.05$, respectively.

FIGURE 1

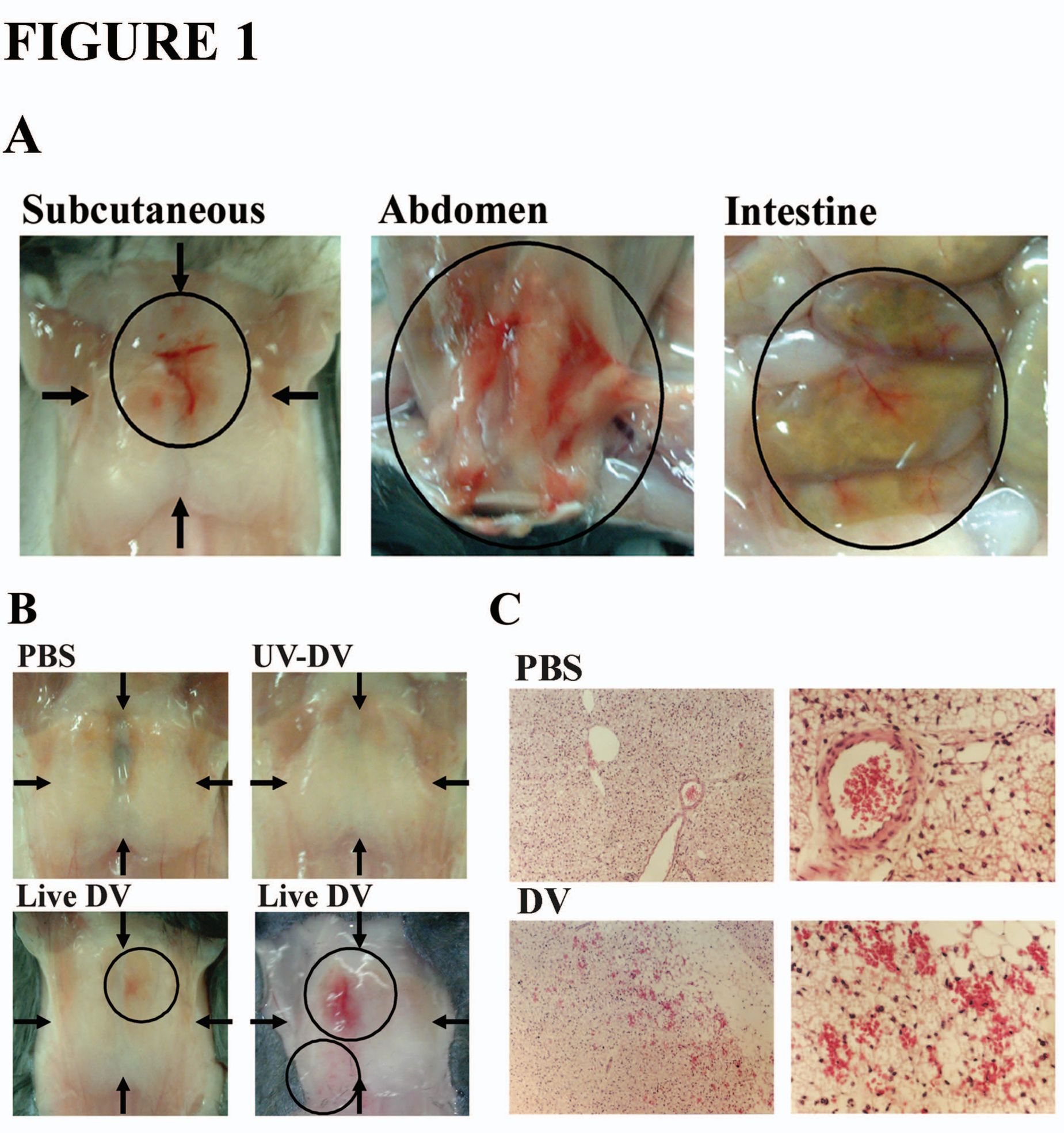
A
Subcutaneous
Abdomen
Intestine
B
PBS
UV-DV
Live DV
Live DV
C
PBS
DV

FIGURE 2

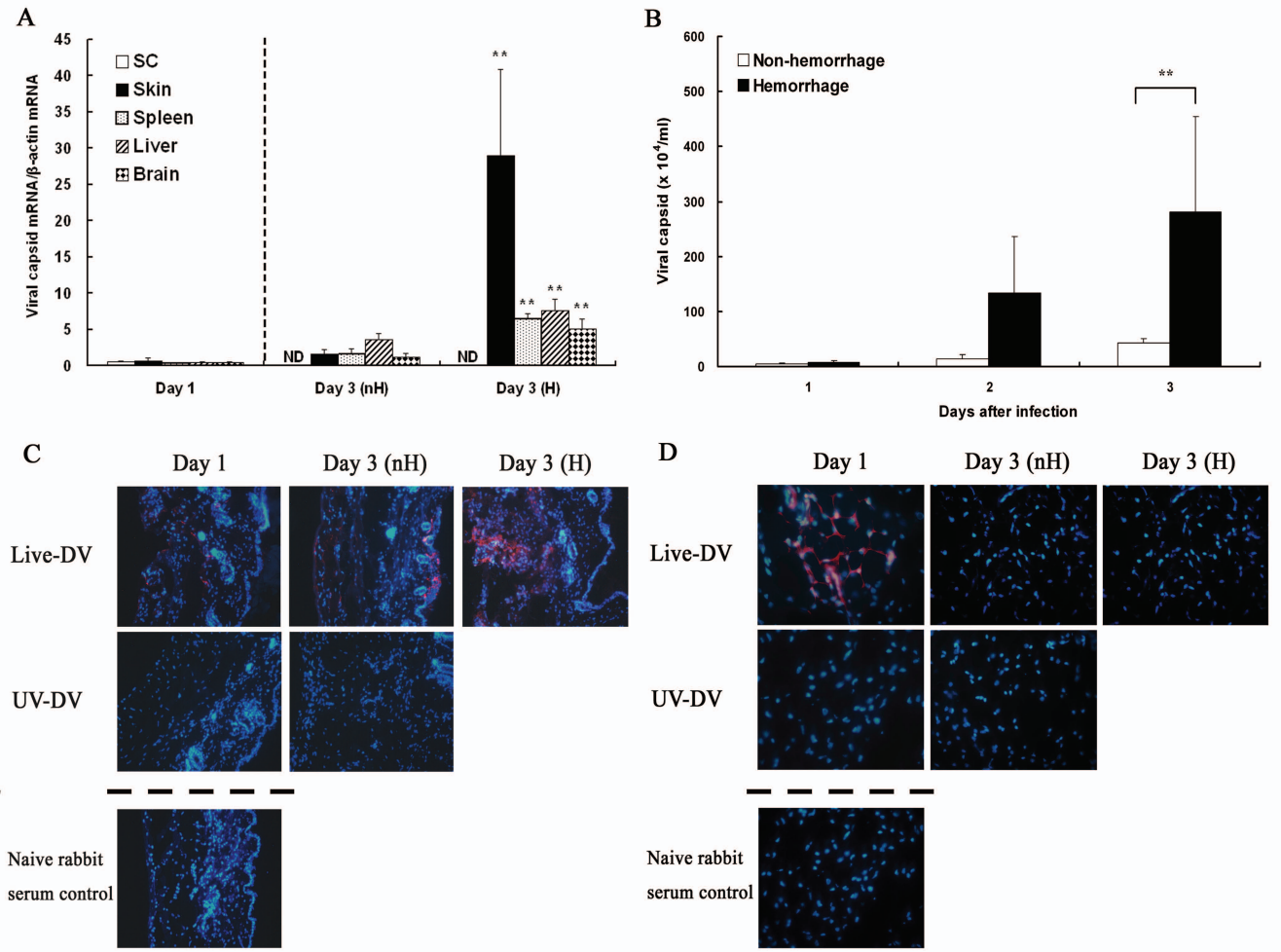
A
Viral capsid mRNA/β-actin mRNA
SC
Skin
Spleen
Liver
Brain
ND
ND
**
Day 1
Day 3 (nH)
Day 3 (H)
B
Non-hemorrhage
Hemorrhage
Viral capsid (x 10⁴/ml)
**
Days after infection
C
Day 1
Day 3 (nH)
Day 3 (H)
Live-DV
UV-DV
Naive rabbit serum control
D
Day 1
Day 3 (nH)
Day 3 (H)
Live-DV
UV-DV
Naive rabbit serum control

FIGURE 3

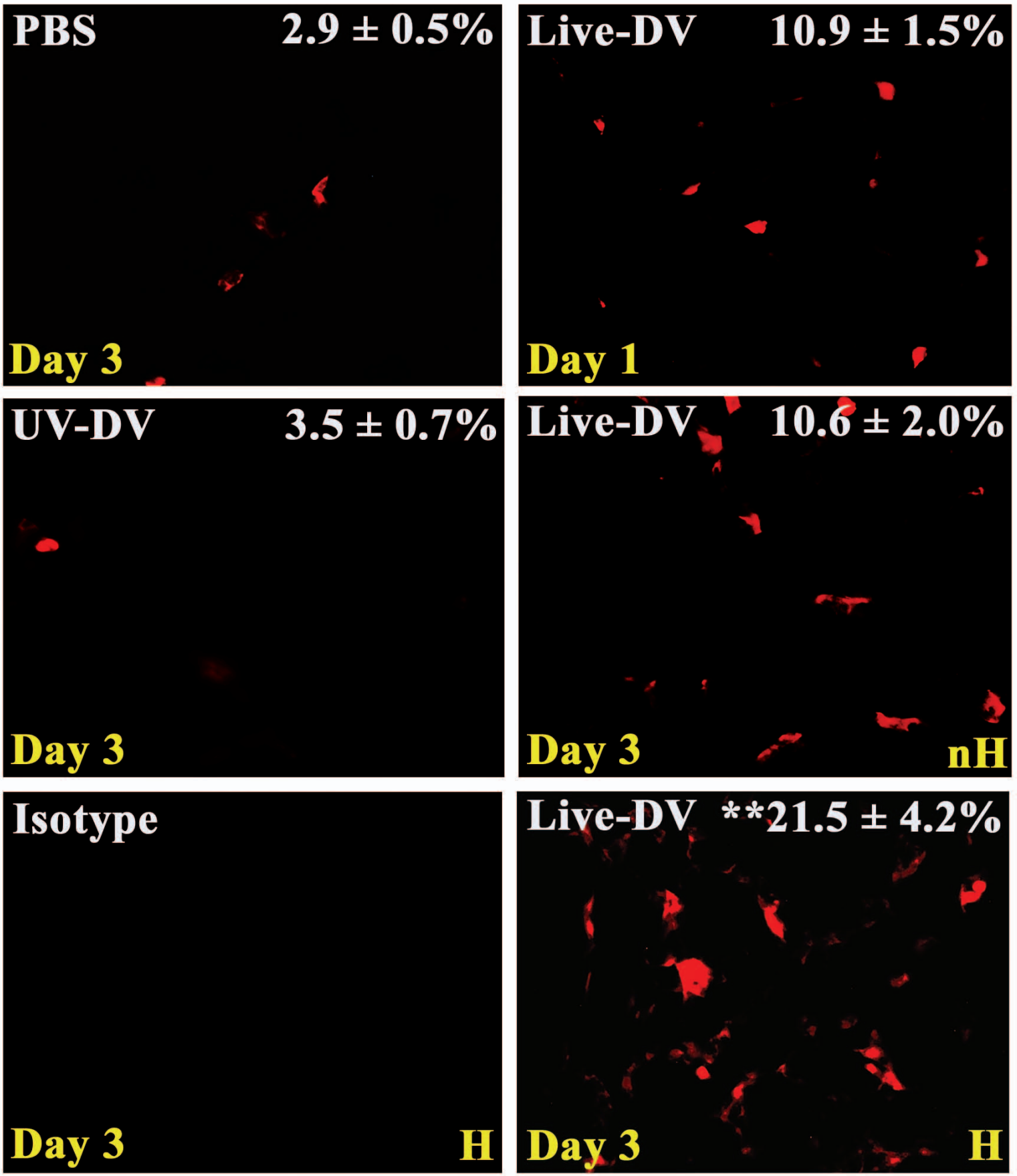
PBS
2.9 ± 0.5%
Day 3
Live-DV
10.9 ± 1.5%
Day 1
UV-DV
3.5 ± 0.7%
Day 3
Live-DV
10.6 ± 2.0%
Day 3
nH
Isotype
Day 3
H
Live-DV
**21.5 ± 4.2%
Day 3
H

FIGURE 4

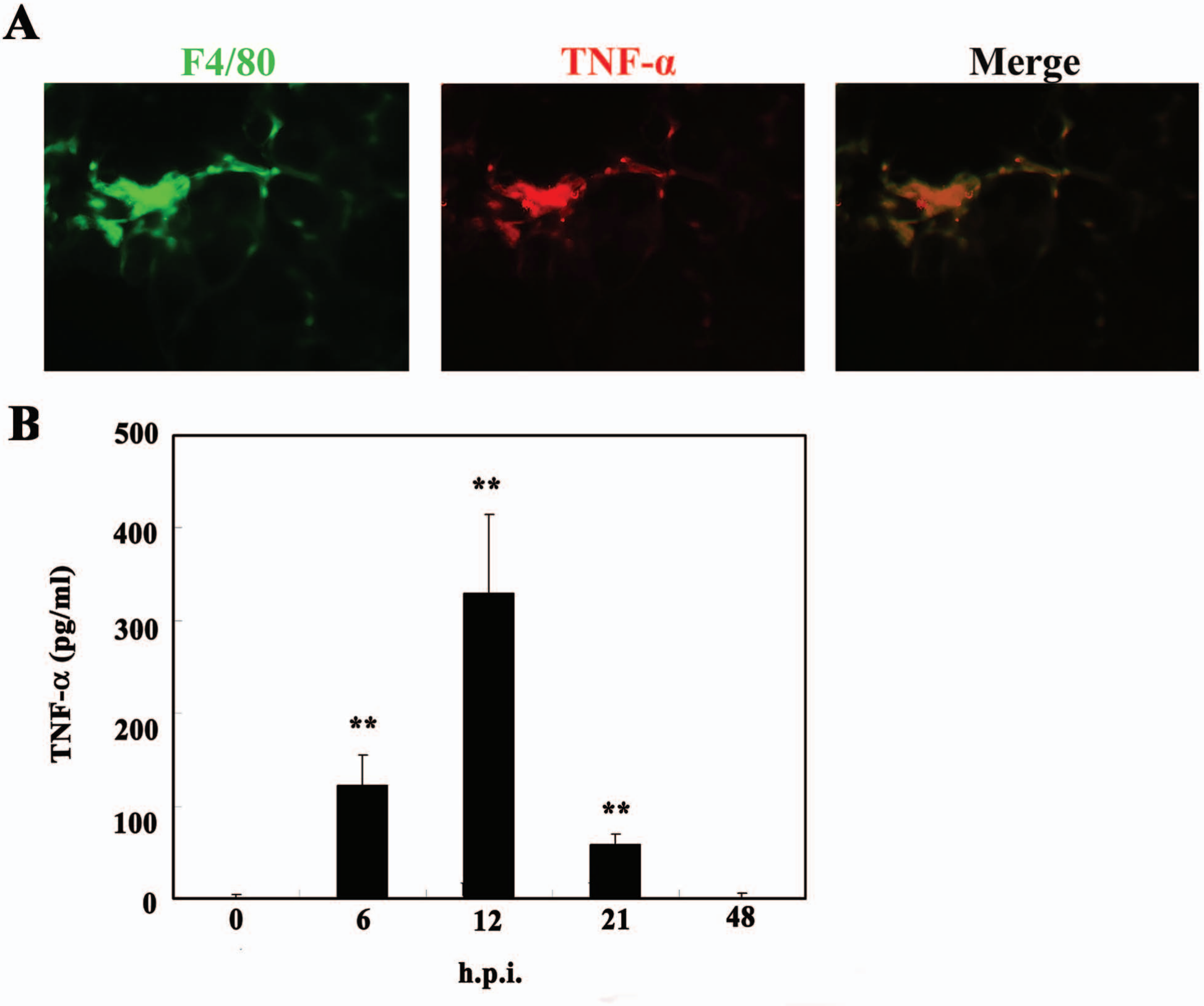
A
F4/80
TNF-α
Merge
B
TNF-α (pg/ml)
500
400
300
200
100
0
**
**
**
0
6
12
21
48
h.p.i.

FIGURE 5

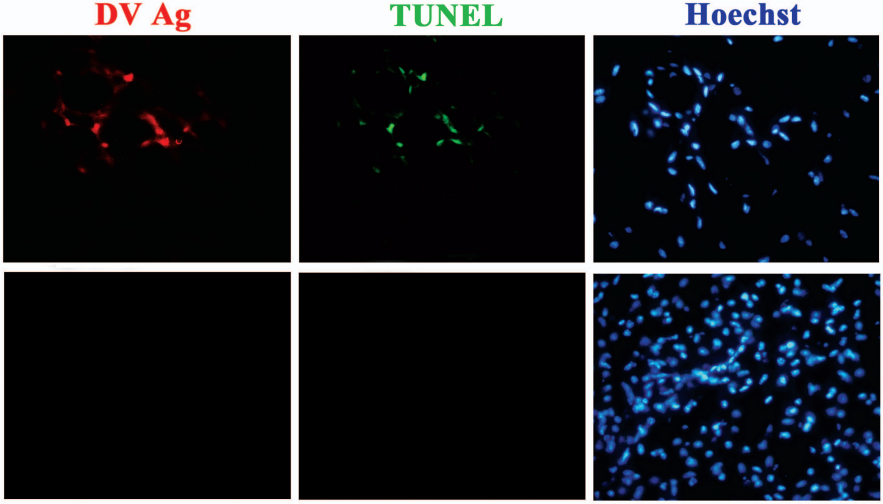

FIGURE 6

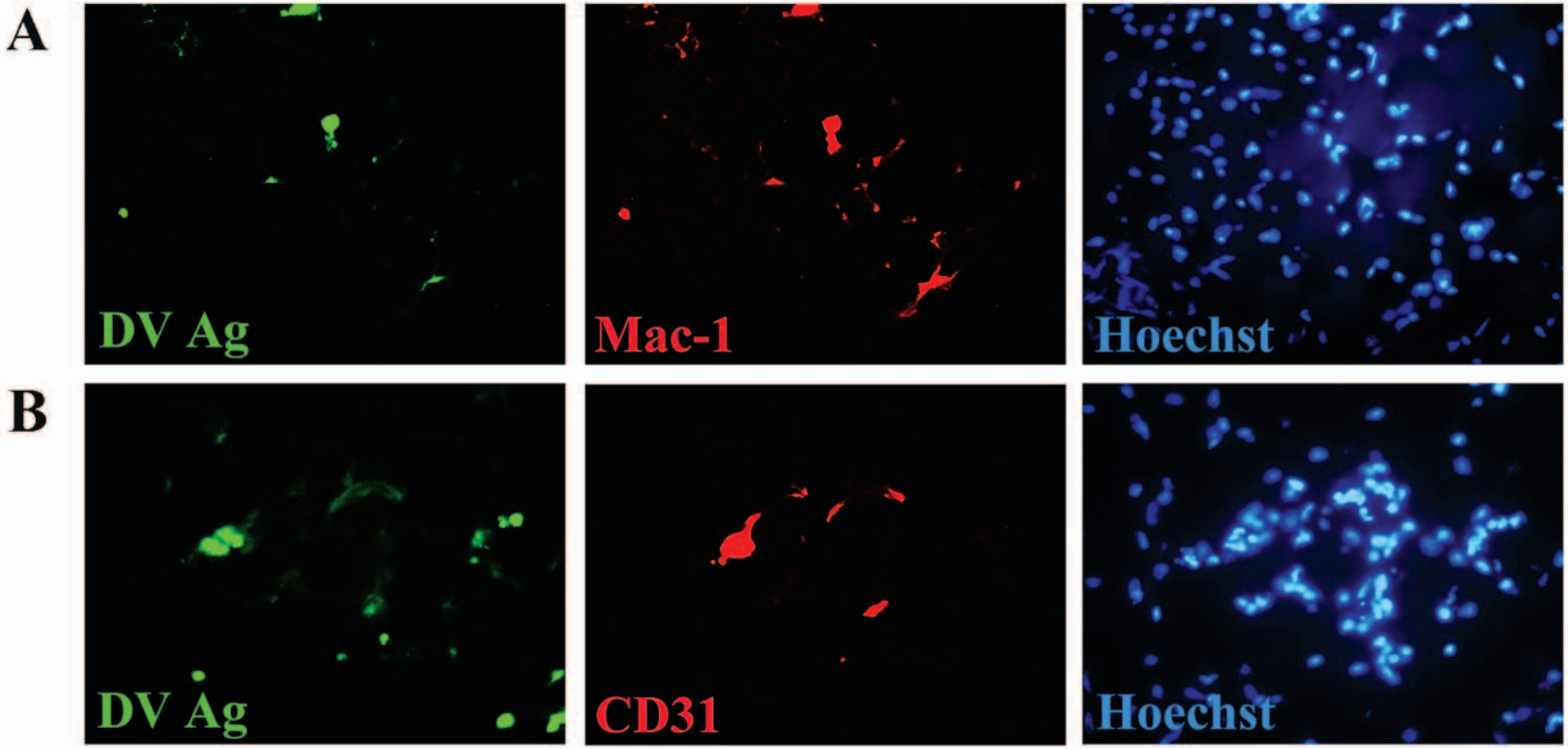

FIGURE 7

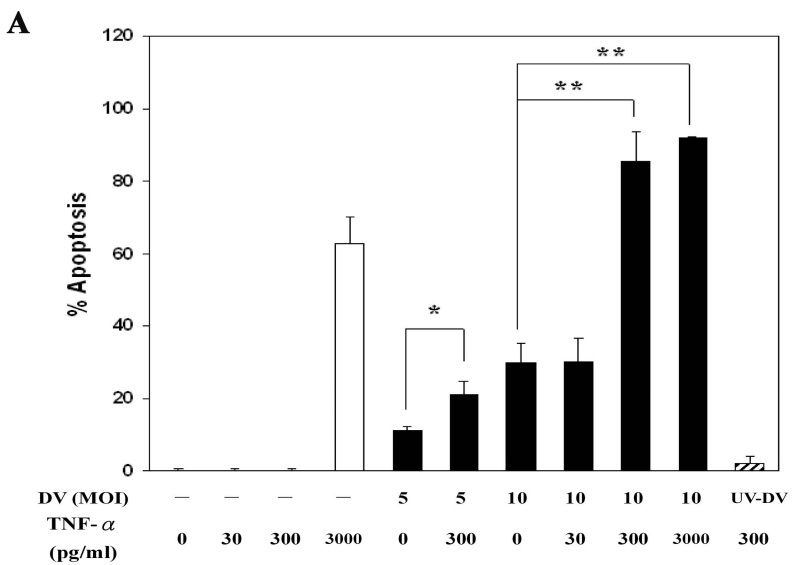
A
% Apoptosis
120
100
80
60
40
20
0
**
**
*
DV (MOI) — — — — 5 5 10 10 10 10 UV-DV
TNF-α (pg/ml) 0 30 300 3000 0 300 0 30 300 3000 300

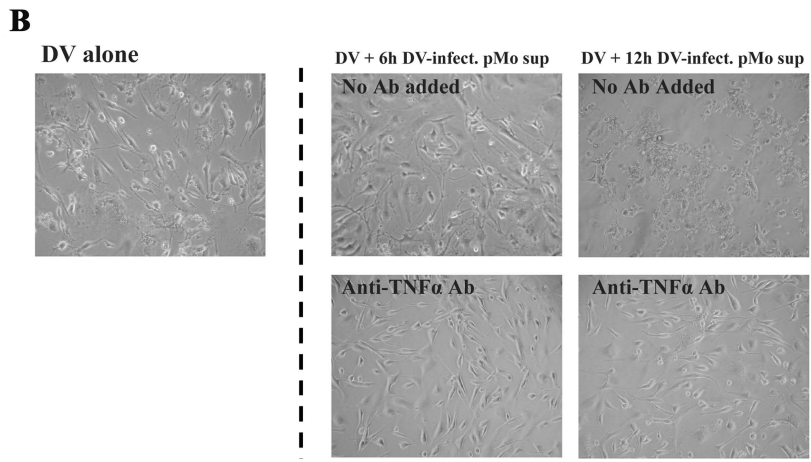
B
DV alone
DV + 6h DV-infect. pMo sup
DV + 12h DV-infect. pMo sup
No Ab added
No Ab Added
Anti-TNFα Ab
Anti-TNFα Ab

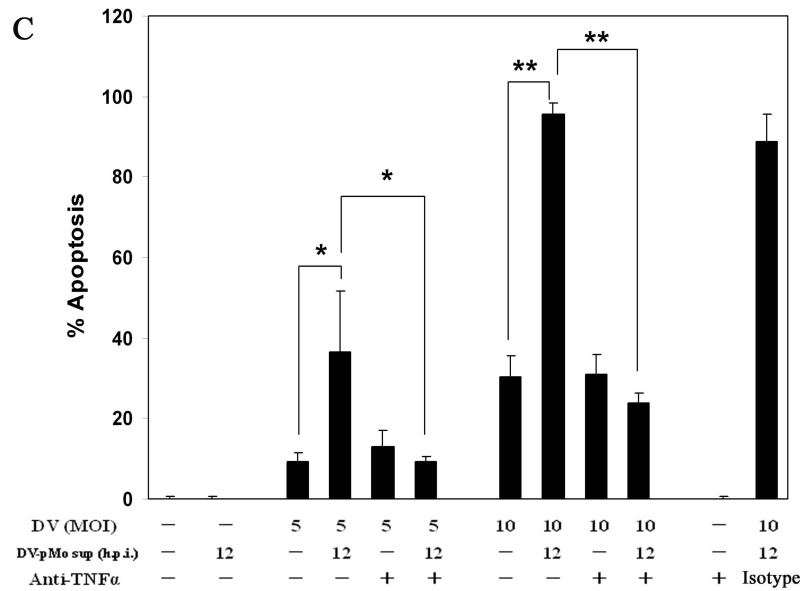
C
% Apoptosis
120
100
80
60
40
20
0
*
*
**
**
DV (MOI) — — 5 5 5 5 10 10 10 10 — 10
DV-pMo sup (h.p.i.) — 12 — 12 — 12 — 12 — 12 — 12
Anti-TNFα — — — — + + — — + + + Isotype